J. Fluid Mech. (1966), *vol.* 25, *part* 4, *pp.* 657–682
Printed in Great Britain

The use of a contraction to improve the isotropy of grid-generated turbulence

By GENEVIÈVE COMTE-BELLOT† AND STANLEY CORRSIN

Mechanics Department, The Johns Hopkins University

(Received 25 October 1965)

It is found that when the average kinetic energies of normal velocity components in decaying, grid-generated turbulence are equilibrated by a symmetric contraction of the wind tunnel, this equality can persist downstream. A second result is further confirmation of the fact that the best power-law fit to the inverse turbulent energy during the early part of decay is near $(x-x_1)^{1.25}$, for both rod grids and disk grids. The Kolmogorov decay law $\sim (t-t_1)^{\frac{10}{7}}$ is re-derived by a spectral method which is essentially equivalent to the original. Finally, a crude theoretical estimate of component energies in the straight duct after a weak contraction seems to support the experiments.

1. Introduction

The use of regular grids in a uniform stream to generate relatively simple turbulence may have begun with the work of Simmons & Salter (1934). Later measurements were made by Dryden, Schubauer, Mock & Skramstad (1937) and Dryden (1943); see also Taylor (1935*b*, part II), Corrsin (1942), Batchelor & Townsend (1947, 1948), Baines & Peterson (1951), Tsuji & Hama (1953), Grant & Nisbet (1957), Wyatt (1955) and others. It is remarkable that in spite of the strongly oriented and inhomogeneous character of the generator, the turbulent motion perhaps 40 or 50 mesh lengths downstream is statistically homogeneous (in planes parallel to the grid) almost within the accuracy of measurements‡ and is approximately isotropic. Since there is no residual mean shear, there is no continuing source of turbulent energy, and the turbulence decays with distance downstream. The rate of this energy decay is very nearly equal to the viscous dissipation rate, and has been one of the continuing objects of theoretical study since the pioneering paper on isotropic turbulence by Taylor (1935*b*).

In order to improve the validity of a comparison between experiments on grid-generated turbulence and theories of isotropic turbulence, it is desirable to improve the degree of isotropy of the former. The spatial inhomogeneity due to decay in the downstream direction must ultimately limit the degree of isotropy attainable. The most obvious measure of anisotropy in the turbulence behind grids is the inequality between the mean-square values of the axial-velocity-

† On leave from the University of Grenoble.

‡ See Corrsin (1963*a*) for remarks on the effects of grid solidity on homogeneity and turbulence level.

component fluctuation $\overline{u^2}$ and any transverse velocity component fluctuation $\overline{v^2} < \overline{u^2}$.

It was pointed out many years ago by Prandtl (1932) and Taylor (1935*a*) that a turbulent motion subjected to gross strain by passage through an axisymmetric area change in a tube will undergo selective changes in its axial and transverse turbulent energy levels due to the directionally selective vortex-line distortions. Their work has been followed up both theoretically and experimentally by a number of people (Ribner & Tucker 1953; Batchelor & Proudman 1954; Townsend 1954; Uberoi 1956; Mills & Corrsin 1959).

A contraction in the tube amplifies relatively the transverse-velocity fluctuations. Consequently, the test section of the wind tunnel we plan to use for grid-turbulence studies includes a slight contraction (area ratio 1·27), roughly chosen on the basis of earlier experiments, to compensate for the observed degree of anisotropy behind grids in uniform channels.

This paper is a report on the performance of this device for making grid-generated turbulence more nearly isotropic, in terms of only the simple measure u'/v'.† Similar experiments have been done by Uberoi & Wallis (1964), who concluded that downstream of the contraction the turbulence tends to return to its original state of anisotropy with u' larger than v'. They suggest that this degree of inequality may be in some way associated with the inhomogeneity in the decaying field.

The experiments reported here had other purposes as well; for example, one was to look for possible differences in the turbulence generated by a grid of square rods and a grid of round rods. Although round rods have been used more commonly, one might expect that square rods would be less sensitive to Reynolds-number variations. On the other hand, Dumas (1964) found that grids with square rods had a tendency to generate large scale oscillatory motions spanning several meshes. To include a case with greater contrast in geometry, we also tested a grid made of flat disks.

Finally, it seemed desirable to make additional measurements of the turbulent-energy decay rate, expecially because the linear law for $1/\overline{u^2}$ recommended by Batchelor & Townsend for the 'initial period' from their data, has not appeared to be the best power-law fit to such experiments.

2. Fluid mechanical apparatus

The wind-tunnel has a closed circuit and a test section 10 m long, about $1 \times 1{\cdot}3$ m in cross-section. The test section walls are sufficiently divergent that no measurable axial gradient in mean speed exists at a speed of 20 m/sec. Over the speed range the empty tunnel 'turbulence' levels (both u'/U_0 and v'/U_0) range from 0·04 to 0·05 % at the upstream end and 0·11 to 0·09 % at the downstream end. These levels are on the tunnel axis. The excess of downstream disturbance over that upstream is presumably due to boundary-layer growth. This conjecture is supported by the downstream reduction at the higher speeds, which

† The prime denotes root-mean-square value.

give thinner boundary layers. The boundary layer was turbulent over this range of speeds.

Temperature fluctuations in the air stream were not detectable, although the mean temperature at the top speed was 10 °C above that outside the tunnel.

The test section and the slight secondary contraction, which is symmetric, are sketched in figure 1. The three possible grid locations are far enough downstream of duct area changes that the mean speed (outside the boundary layers) is uniform within the accuracy of measurement.

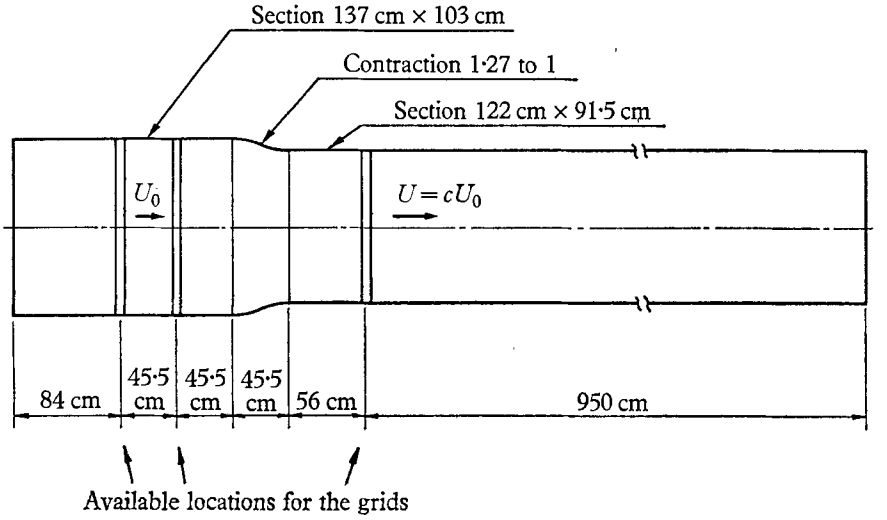

FIGURE 1. Sketch of wind-tunnel test section, including contraction giving axially symmetric strain.

The turbulence-generating grids were of three types:

(1) a biplane group with square mesh, square rods;

(2) a single biplane grid with square mesh but round rods;

(3) a single square-mesh grid of round disks.

The first group were all of solidity (projected solid area per unit total area) $\sigma = 0{\cdot}34$, with mesh sizes (distance between rod centre lines) $M = 2{\cdot}54$ cm, 5·08 cm and 10·16 cm. The single round-rod grid was included to provide a check with earlier studies, which used primarily this configuration. It had $M = 5{\cdot}08$ cm but $\sigma = 0{\cdot}44$. The intent was to have approximately the same pressure-drop coefficient, hence turbulence level, as the 5·08 cm square-rod grid (Corrsin 1963*a*). It fell a bit short; a higher σ would have risked general instability. The disk grid had $M = 5{\cdot}08$ cm and $\sigma \simeq \frac{1}{10}\pi$. Experiments were run on the collection of square-rod grids over a range of Reynolds numbers ($R_M \equiv U_0 M/\nu$) from $1{\cdot}7 \times 10^4$ to $1{\cdot}35 \times 10^5$. U_0 is mean speed for the same mass flow rate in the empty part of the tunnel. Each grid was made in two sizes, one to fit upstream of the slight secondary contraction, the other to fit downstream.

The square rods for the 2·54 cm grid were of polished brass. All other rods were of polished dural. Rod crossings were pinned. The disks were 0·080 cm thick and were glued to the intersections of a square-mesh array of 0·084 cm piano wire.

3. Measuring equipment and procedure

All data were taken with platinum–(10 %) rhodium hot-wire anemometers, 3·5 microns in diameter, about 0·4 mm long, etched from Wollaston after being soldered to the tips of jewellers' broaches. Most measurements of axial turbulent-velocity component u were made with a single wire set normal to the mean flow. The static sensitivity to u-fluctuations was determined directly by the local tangent of the empirical curve of voltage versus velocity. The air temperature was maintained constant to within $\pm 0{\cdot}1$ °C during calibration.

The transverse velocity component v was measured with an X-meter.† The (inevitably) slightly different wires were subjected to enough difference in heating current to match their time constants. In such devices the simple voltage difference, independent of u in an ideally symmetric meter, is dependent on u as well as on the primary input v. Therefore a weighted voltage difference is formed $(e_1 - Ke_2)$, where K is the ratio of the two u-sensitivities. This weighted difference is then empirically related to v by rotating the X-meter through a small angle in the 'plane' of the X, and measuring $(e_1 - Ke_2)$ as a function of angle.

Some check measurements of u' were made with the X-meter. In this case the ideal meter yields u from the voltage sum $(e_1 + e_2)$. For a real meter the parasitic response of $(e_1 + e_2)$ to v is avoided by forming the weighted sum $(e_1 + K'e_2)$, where K' is the ratio of the two v-sensitivities. The foregoing procedures are described more explicitly by Comte-Bellot & Mathieu (1958) and Comte-Bellot (1960).

The parasitic response of the X-meter to w-fluctuations was negligible for both sum and difference operations. In addition to the cross-responses, we ordinarily must take account of the effect of one velocity component in changing the *sensitivity* of the hot-wire array to the 'primary' component for each configuration. This effect is negligible in grid turbulence because the orthogonal components are uncorrelated.

The basic electrical and electronic circuitry for the hot-wires was a Shapiro and Edwards constant-current unit. All turbulence levels were measured with the high-frequency cut-off set at a nominal value of 20,000 cycles/sec and the low-frequency cut-off at 1 cycle/sec. Compensation-circuit settings were determined with the built-in square-wave generator. Output signals were squared and averaged with the built-in vacuum thermocouple and galvanometer.

Corrections for finite hot-wire length were negligible in the data reported here. Corrections for background (no grid) turbulence, for possible air-temperature fluctuations and for electronic noise were all made by subtracting from the mean square total signal the mean square signal in the empty tunnel at the same position, speed and hot-wire condition. This is rather *ad hoc* for the first of these three effects because it assumes that the extraneous contributions are uncorrelated with the primary turbulence under study. The correction was negligible in all cases except the large $U_0 t/M$ region behind the 2·54 cm grids, where it reached a maximum of 3 %, t is travel time, grid to hot wire.

The repeatability of the u' or v' values in a single run is estimated as within ± 2 %. Figure 6 shows little scatter on individual curves. On the other hand, the

† For all cases $\overline{w^2} = \overline{v^2}$ within the accuracy of measurement.

absolute level of a curve varied from day to day by as much as $\pm 4\,\%$. In order to minimize this effect (most likely a reflexion of inaccuracies in calibration for u- or v-sensitivity), each run was accompanied by measurement of a 'standard case' at each speed, and the absolute level was determined relative to this standard. For example, in the runs with $U_0 = 20$ m/sec, a standard was u' and v' at $U_0 t/M = 42$ behind the 5·08 cm, square-rod grid upstream of the contraction. The values of u'/U_0 and v'/U_0 at this point were determined with relatively good precision by taking arithmetic means over ten measurements.

4. Straight duct

4.1. *Component turbulent energies*

All biplane grids generated turbulence which was laterally homogeneous within the accuracy of measurement for $x/M > 40$. x is the axial distance behind the grid, M is the grid mesh. For *relative* measurements involved in checking lateral homogeneity at fixed x, the accuracy is estimated as $\pm 1\,\%$ rather than the value $\pm 2\,\%$ indicated for the 'absolute' turbulence-level determinations. Wall effects reduced the domain of lateral homogeneity to 16 in. × 28 in. far downstream, at $U_0 t/M = 165$ for the $M = 2$ in. grids.

This turbulence field is appreciably more homogeneous than that reported by Grant & Nisbet (1957) and somewhat more homogeneous than that obtained earlier with wooden rods (e.g. Corrsin 1942), metal rods (Corrsin 1963*a*) or metallic heating rods (Mills & Corrsin 1959). Manufacturing precision of the grids is indicated by the central 24 in. × 24 in. of the 5·08 cm mesh, square-rod grid; a maximum departure from mean gap width of $\pm 0{\cdot}7\,\%$. The rods were uniform to within $\pm 0{\cdot}8\,\%$ maximum departure. The standard deviations were considerably smaller.

The first result of interest here is the degree of inequality of turbulence components in the streamwise (axial) and transverse directions. A convenient measure is $(u'/v') - 1$. Figures 2, 3 and 4 show u'/v' versus $U_0 t/M$ for the various grids. $U_0 t/M$, a dimensionless time, is used instead of x/M to permit more direct comparison with the abscissae of similar plots for cases with a stream contraction, hence different U_0 for equal grid Reynolds number.

Figure 2 collects the principal new results on u'/v' behind square-mesh, square-rod, biplane grids in a straight duct. The data for $U_0 t/M > 40$, the region of lateral homogeneity, are especially relevant. Consistent with most earlier reports, the axial-turbulence intensity is slightly greater than the transverse, there is a trend toward equality, and there is a possible but not unequivocal dependence on Reynolds number. The trend toward equality is so slow that, if extrapolated, it yields $u' = v'$ where the turbulence is in its 'final' (non-inertial, small Reynolds number) period. This extrapolation is, of course, not physically valid that far. Batchelor & Stewart (1950) have shown that far downstream behind a grid in a straight duct the strongly anisotropic largest 'eddies' (which have the longest relaxation times) are the dominant residuum.

Figures 3 and 4 show basically the same character for u'/v' behind the round-rod grid at two Reynolds numbers and the disk grid. Figure 5 compares one data

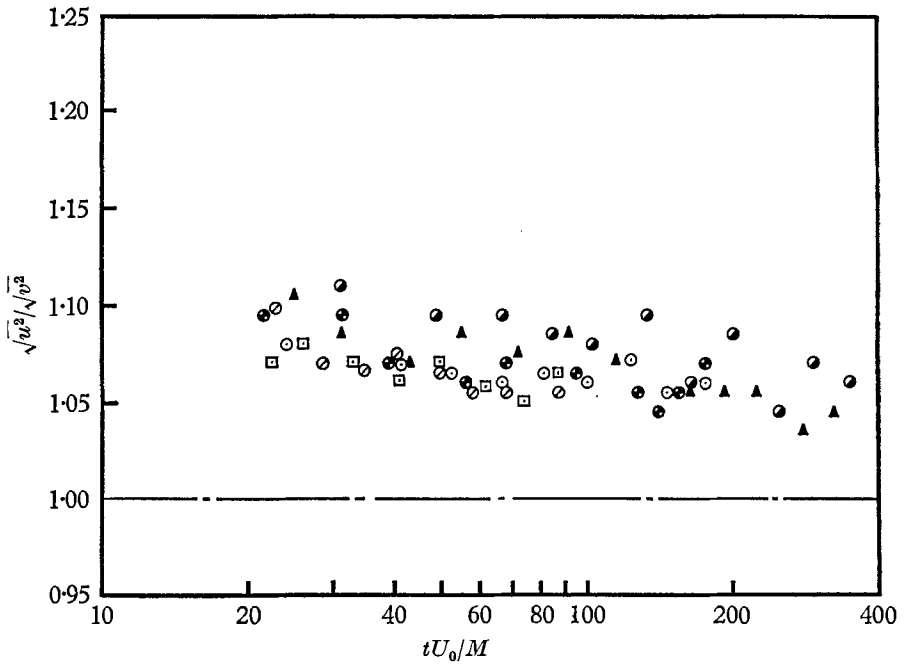

FIGURE 2. Anisotropy of grid-generated turbulence without contraction—biplane, square-grids. ▲, $U_0 = 10$ m/sec, $M = 2{\cdot}54$ cm; ◕, $U_0 = 10$ m/sec, $M = 5{\cdot}08$ cm; ⌀, $U_0 = 10$ m/sec, $M = 10{\cdot}16$ cm; ◕, $U_0 = 20$ m/sec, $M = 2{\cdot}54$ cm; ○, $U_0 = 20$ m/sec, $M = 5{\cdot}08$ cm; □, $U_0 = 20$ m/sec, $M = 10{\cdot}16$ cm.

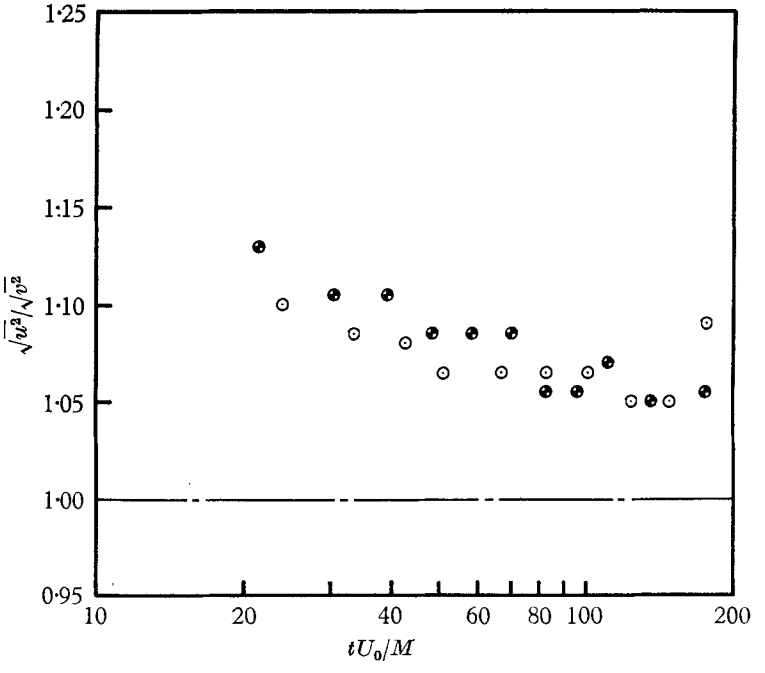

FIGURE 3. Anisotropy of grid-generated turbulence without contraction—biplane, round-rod grids, $M = 5{\cdot}08$ cm. ◕, $U_0 = 10$ m/sec; ⊙, $U_0 = 20$ m/sec.

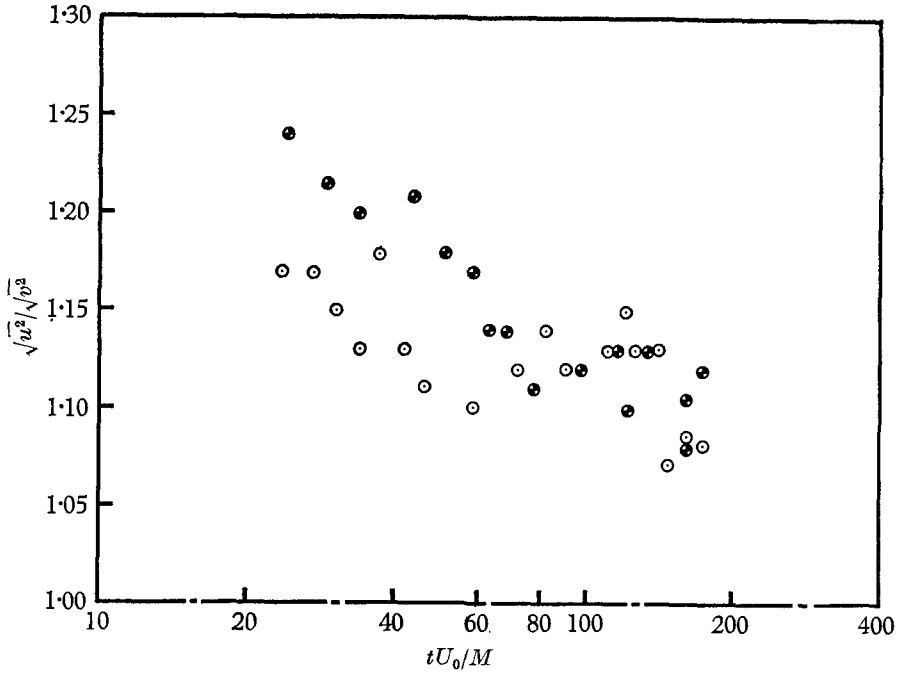

FIGURE 4. Anisotropy of grid-generated turbulence without contraction—disk grid, M = 5·08 cm. ◕, U_0 = 10 m/sec; ⊙, U_0 = 20 m/sec.

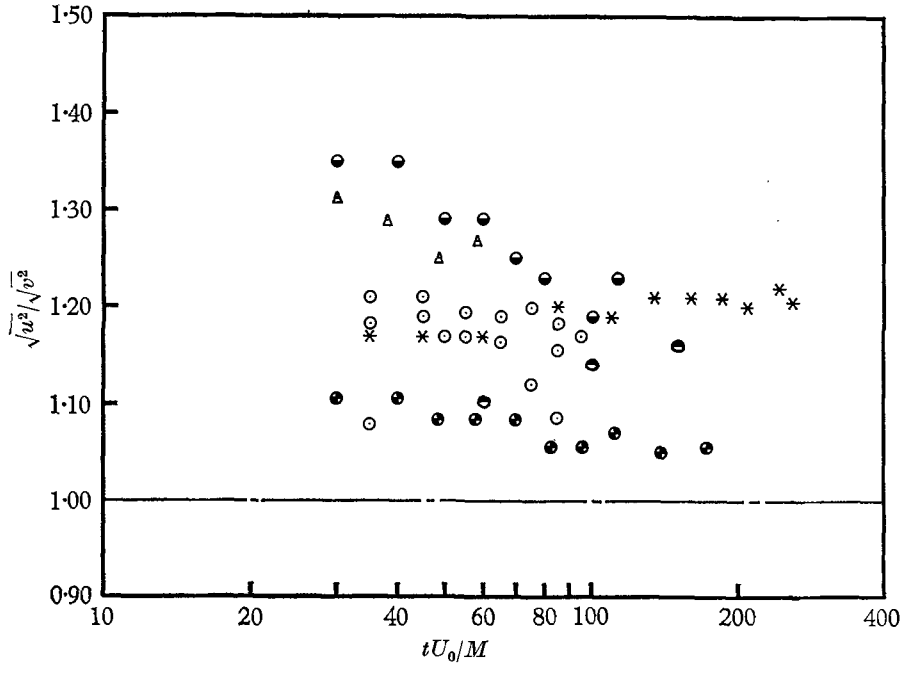

FIGURE 5. Anisotropy of grid-generated turbulence without contraction—comparison with some earlier round-rod-grid experiments. ◓, ◒, Corrsin (1942); ⊙, Wyatt (1955); △, Kistler & Vrebalovich (1961); ∗, Uberoi (1963); ◕, present authors.

set of figure 3 with some earlier results behind round rod grids. The range of anisotropies $(u'/v') - 1$ is considerable, but it is always of the same sign.

4.2. *Decay rates*

It has long been customary to try to fit grid-turbulence-decay data with power laws over various periods during the lifetime of the turbulence. Power laws are not only analytically convenient, but also, since they are the forms most easily deduced by dimensional arguments, they make a nice target for theoretical analysis based on this simplest of techniques.

Therefore, following for example Batchelor & Townsend, we try to find the best power laws for the data on $1/\overline{u^2}$ and $1/\overline{v^2}$. Since the actual grid location is irrelevant in the fully developed range, we use the empirical forms

$$\frac{U_0^2}{\overline{u^2}} = A_1\left(\frac{U_0 t}{M} - \frac{U_0 t_1}{M}\right)^{n_1}, \tag{1}$$

$$\frac{U_0^2}{\overline{v^2}} = A_2\left(\frac{U_0 t}{M} - \frac{U_0 t_2}{M}\right)^{n_2}. \tag{2}$$

Since $\overline{v^2} \neq \overline{u^2}$, there is little reason to use the same effective origin for both components. The procedure was to plot (1) and (2) on log paper and try ranges of values for t_1 and t_2, seeking for each set of data the values which gave the longest straight lines. The slopes of these lines determined n_1 and n_2, while the ordinate levels determined A_1 and A_2. A typical case, with 'optimum' effective origins, is presented in figure 6. Obviously there is a slow approach toward equality. It is also interesting that the independently determined effective origins for the two power laws are virtually the same. A tabulation of the empirical constants in equations (1) and (2) for a number of cases is presented in table 1. The brackets around some of the A_1 and A_2 values indicate three runs for which we neglected to check hot-wire sensitivities by comparison with the 'standard' case. Therefor A_1 and A_2 are there subject to the full $\pm 4\,\%$ uncertainty.

In all cases (see figures 2 and 3) $\overline{u^2} > \overline{v^2}$, and in all cases the two curves are very slowly approaching each other with increasing $U_0 t/M \equiv x/M$. There is little difference between the round-rod and square-rod cases. Even the round-disk-grid data show the same general character. The estimated uncertainties in $U_0 t_{1,2}/M$ are about $\pm 1{\cdot}0$, and that in determining the exponents $n_{1,2}$ is about $\pm 0{\cdot}02$.

For the square-rod-grid geometry there is little trend with Reynolds number over the test range of 8 : 1 (a slight decrease in n_1 and increases in t_1, A_1 and A_2 are beyond the scatter). The two repeated experiments indicate the magnitude of the scatter. There is slightly more disagreement between pairs of cases in which equal Reynolds numbers were obtained with different M. This may reflect differences in manufacturing precision of the grids or effects of tunnel operation at different speeds (such as free-stream or boundary-layer state).

As a quantitative measure of the rate of approach to component equality $\overline{u^2}/\overline{v^2} \to 1$, we might select

$$\frac{1}{(u'/v') - 1}\frac{d}{d(U_0 t/L_f)}\{(u'/v') - 1\}, \tag{3}$$

or, since there are no extensive data on L_f, the integral scale of axial turbulence component in the axial direction (see equation (27)),

$$\frac{1}{(u'/v')-1}\frac{d}{d(U_0t/M)}\{(u'/v')-1\}. \tag{4}$$

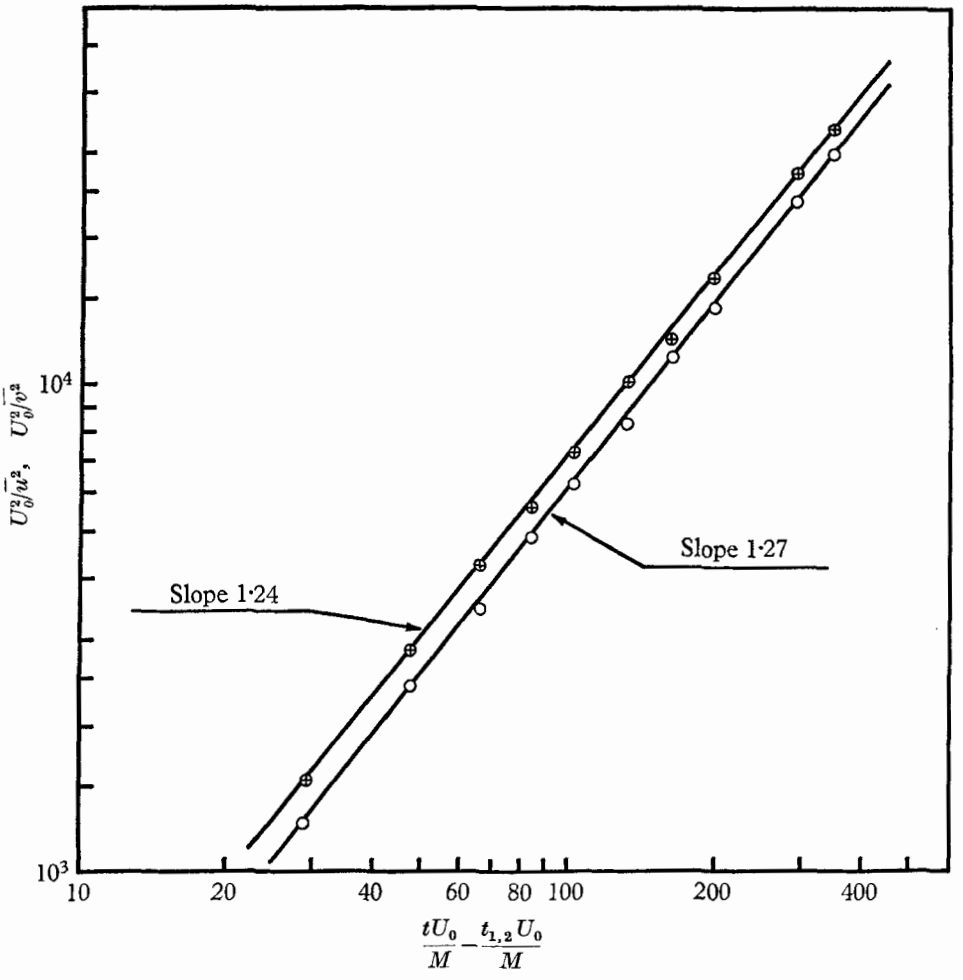

FIGURE 6. Example of u' and v' decay for a square-rod grid with $M = 2{\cdot}54$ cm, $U_0 = 20$ m/sec and without contraction. ○, $U_0^2/\overline{u^2}$ with $t_1U_0/M = 2.5$; ⊕, $U_0^2/\overline{v^2}$ with $t_2U_0/M = 2$.

These values are highly scattered but all negative and of magnitude very much less than unity. We infer an approach toward isotropy, though a very slow one. Extrapolation of these empirical power-law curves to $u' = v'$ gives U_0t/M values ranging from roughly a thousand to a hundred thousand, but no clear trends in terms of grid geometry or Reynolds number.

Table 2 presents some of the same kinds of data as those in table 1, but for several earlier investigations. Notable differences from the present results are the

equality of $\overline{u^2}$ and $\overline{v^2}$ in the results of Batchelor & Townsend (in a sense later amended by Grant & Nisbet 1957), and the values $n_1 = n_2 = 1{\cdot}0$ determined from the data of Kistler & Vrebalovich (1961).

		Grid			$\overline{u^2}$-decay			$\overline{v^2}$-decay		
R_M ($\times 10^{-3}$)	U_0 (m/sec)	M (cm)	σ	Type	n_1	$\frac{U_0 t_1}{M}$	A_1	n_2	$\frac{U_0 t_2}{M}$	A_2
17	10	2·54	0·34	Biplane, square rods	1·33	1·5	13	1·27	1·5	20
34	20				1·27	2·5	18	1·24	2	23
29	8·5	5·08	0·34	Biplane, square rods	1·27	2·5	(16)	1·21	3	(24)
34	10				1·26	3	17	1·20	3	25
34	10	—	—	—	1·25	3	18	1·23	2·5	22
68	20	—	—	—	1·27	3	(15)	1·23	2·5	(23)
68	20	—	—	—	1·24	3	21	1·23	2·5	24
92	27	—	—	—	1·22	4	(21)	1·19	3	(28)
68	10	10·16	0·34	Biplane, square rods	1·19	4	22	1·18	3	26
135	20				1·18	3·5	22	1·16	3	27
34	10	5·08	0·44	Biplane, round rods	1·30	2	23	1·24	2	37
68	20				1·27	2	27	1·26	2	33
34	10	5·08	0·31	Disks	1·33	6	5·9	1·32	2·5	7·5
68	20				1·39	2	4·2	1·36	5	6·2

TABLE 1. Energy decay of grid turbulence

			Biplane grids			$\overline{u^2}$-decay			$\overline{v^2}$-decay		
Reference	R_M ($\times 10^{-3}$)	U_0 (m/sec)	M	σ	Rods	n_1	$\frac{U_0 t_1}{M}$	A_1	n_2	$\frac{U_0 t_2}{M}$	A_2
Corrsin (1942)	8·5	10·0	1·27 cm	0·44	Rd.	1·30	1	20	1·22	1·5	59
	17	10·0	2·54	0·44	Rd.	1·28	3	23	1·14	2·5	62
	26	15·0	2·54	0·44	Rd.	1·35	1	17	1·16	1	58
Batchelor & Townsend (1947, 1948)	5·5	6·43	1·27	0·34	Rd.	1·13	5	70	—	—	—
	11	12·86	1·27	0·34	Rd.	1·25	8	48	—	—	—
Baines & Petersen (1951)	24	8	4·45	0·44	Sq.	1·37	3	8·5	—	—	—
Tsuji & Hama (1953)	33	10	5·0	0·36	Rd.	1·35	0	10	—	—	—
Wyatt (1955)	11	6·25	2·54	0·34	Rd.	1·27	5	31	$\approx n_1 \approx \frac{U_0 t_1}{M} \approx 1{\cdot}3A_1$		
	22	12·5	2·54	0·34	Rd.	1·27	3·5	35			
	44	12·5	5·08	0·34	Rd.	1·25	4	35			
Kistler & Vrebalovich (1961)	2420	66 ($p = 4$ atm)	17·1	0·34	Rd.	1·0	9	71	1·0	7	110
Uberoi (1963)	29	17	2·54	0·44	Rd.	1·20	4	24	1·20	4	35

TABLE 2. Analysis of some previous decay results in terms of a power law

5. Slight contraction

5.1. *Component energies*

Assuming u'/v' values like those in table 2, our wind tunnel was designed with a slight secondary contraction (figure 1) with area ratio $c = 1{\cdot}27$ based on the data of Uberoi (1956) and of Mills & Corrsin (1959), to give $u' \approx v'$ after the strain.

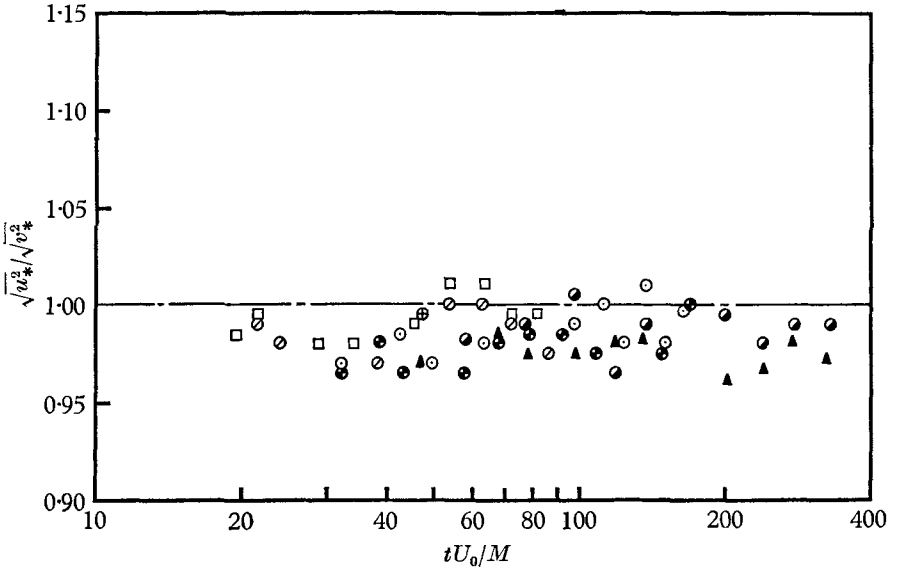

FIGURE 7. Effect of 1·27:1 contraction on the anisotropies of figure 2 (square rods). ▲, $U_0 = 10$ m/sec, $M = 2{\cdot}54$ cm; ◔, $U_0 = 10$ m/sec, $M = 5{\cdot}08$ cm; ∅, $U_0 = 10$ m/sec, $M = 10{\cdot}16$ cm; ◕, $U_0 = 20$ m/sec, $M = 2{\cdot}54$ cm; ○, $U_0 = 20$ m/sec, $M = 5{\cdot}08$ cm; □, $U_0 = 20$ m/sec, $M = 10{\cdot}16$ cm. Contraction at $9M$ or $18M$ (table 3).

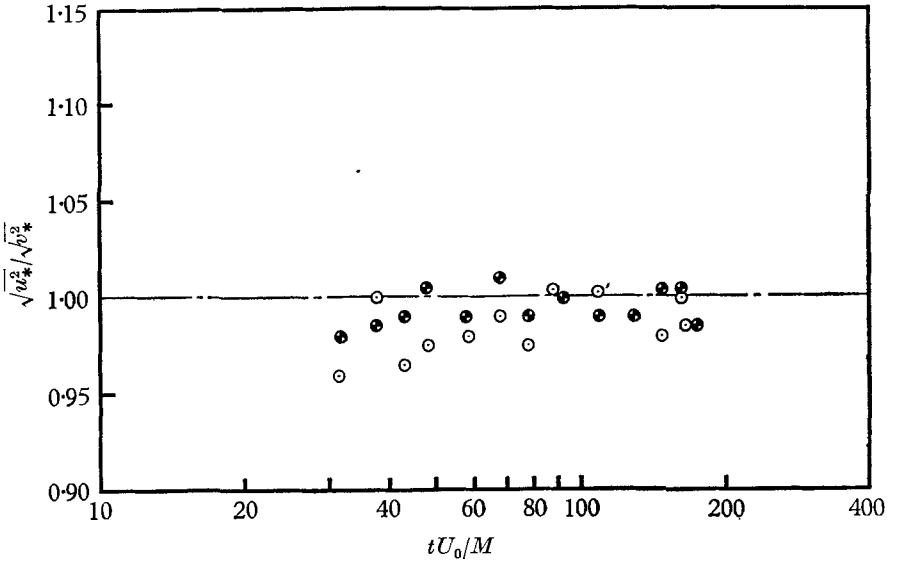

FIGURE 8. Effect of 1·27:1 contraction on the anisotropies of figure 3 (round rods, $M = 5{\cdot}08$ cm). ◔, $U_0 = 10$ m/sec; ⊙, $U_0 = 20$ m/sec. Contraction at $18M$.

Of course, a single area ratio cannot be correct for all grid geometries, all grid positions and all Reynolds numbers, but the results in figures 7–11 show that for several cases this particular area ratio is satisfactory. In no case here does the

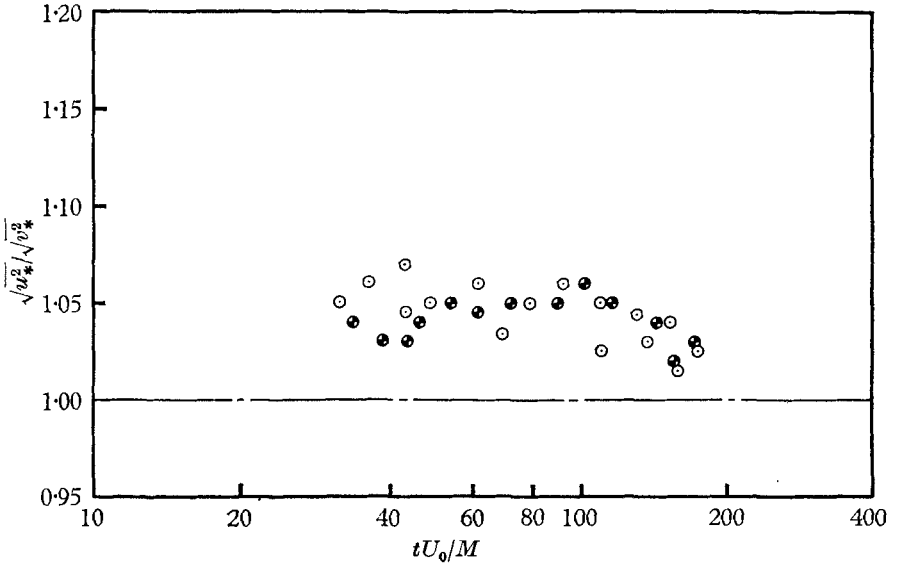

FIGURE 9. Effect of 1·27:1 contraction at $18M$ on the anisotropies of figure 4 (disks, $M = 5{\cdot}08$ cm). ◓, $U_0 = 10$ m/sec; ⊙, $U_0 = 20$ m/sec.

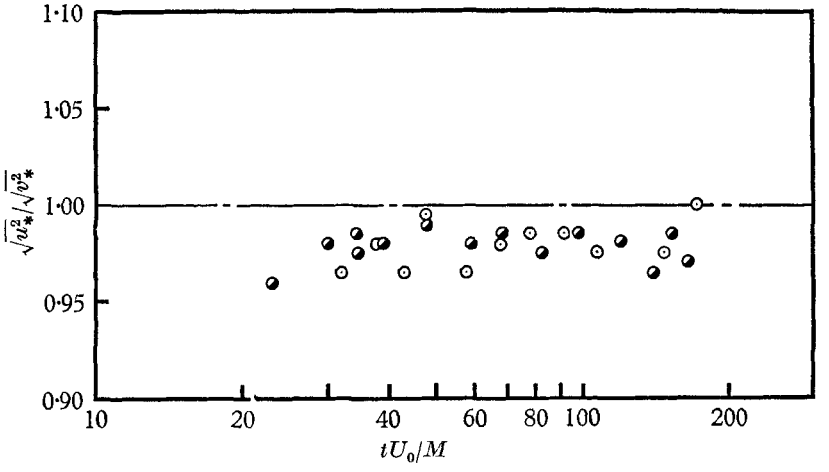

FIGURE 10. Effect of contraction position on downstream anisotropy for square rods with $M = 5{\cdot}08$ cm, $U_0 = 10$ m/sec. ◕, Contraction at $9M$; ⊙, contraction at $18M$.

average u'/v' depart from unity by more than 5 %. Figure 7 is intended to show primarily the possible dependence on Reynolds number. Four cases have the contraction located at $U_0t/M = 18$. With the largest grid this was not convenient, so it is relatively closer to the contraction, $U_0t/M = 9$. Figures 8 and 9 show the round-rod and disk-grid results at two Reynolds numbers.

Perhaps the most noteworthy result in these data is the absence of a return to $u'/v' > 1$ with increasing x. This is at variance with some results of Uberoi (1965), who reported a clear tendency of his strained turbulence (with $u'/v' < 1$) to return to the pre-contraction condition, $u'/v' > 1$.

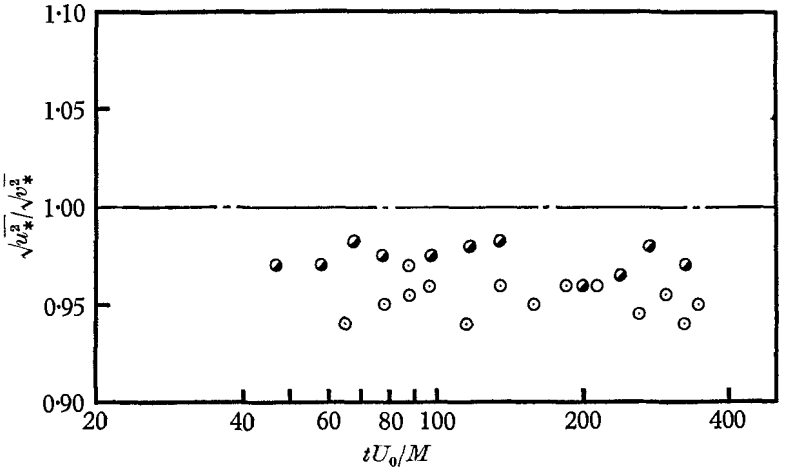

FIGURE 11. Effect of contraction position on downstream anisotropy for square rods with $M = 2{\cdot}54$ cm, $U_0 = 10$ m/sec. ◕, Contraction at $18M$; ⊙, contraction at $36M$.

5.2. *Decay rates*

As for the straight duct, the decay data were empirically fitted by best power laws for $1/\overline{u^2}$ and $1/\overline{v^2}$:

$$\frac{U_0^2}{\overline{u^2}} = A_1^* \left(\frac{U_0 t}{M} - \frac{U_0 t^*}{M}\right)^{n_1^*}, \tag{5}$$

$$\frac{U_0^2}{\overline{v^2}} = A_2^* \left(\frac{U_0 t}{M} - \frac{U_0 t^*}{M}\right)^{n_2^*}. \tag{6}$$

In contrast to equations (1) and (2), these curves have been given the same effective origin, because the energies are more nearly equal. Attempts to select separate origins empirically led to no significant differences.

Figure 12 shows a typical experiment in which $\overline{u^2} \approx \overline{v^2}$ immediately after straining. The equality persists. Table 3 summarizes the several cases studied. The values of the exponents n_1^* and n_2^* are essentially equal to each other and are roughly the same as in the straight duct, except for the cases with the contraction located at $U_0 t/M = 9$. These latter include the largest-Reynolds-number case, but the difference does not appear to be a Reynolds-number effect because the cases of $R_M = 68 \times 10^3$ with the 5·08 cm grids and $R_M = 68 \times 10^3$ with the 10·16 cm grid (with contraction at $U_0 t/M = 18$) are different from each other.

For the experiments with contraction, the elapsed time is calculated from

$$t = \int \frac{dx}{\overline{U}(x)}. \tag{7}$$

U_0 is mean speed in the empty part of the duct approaching the grid.

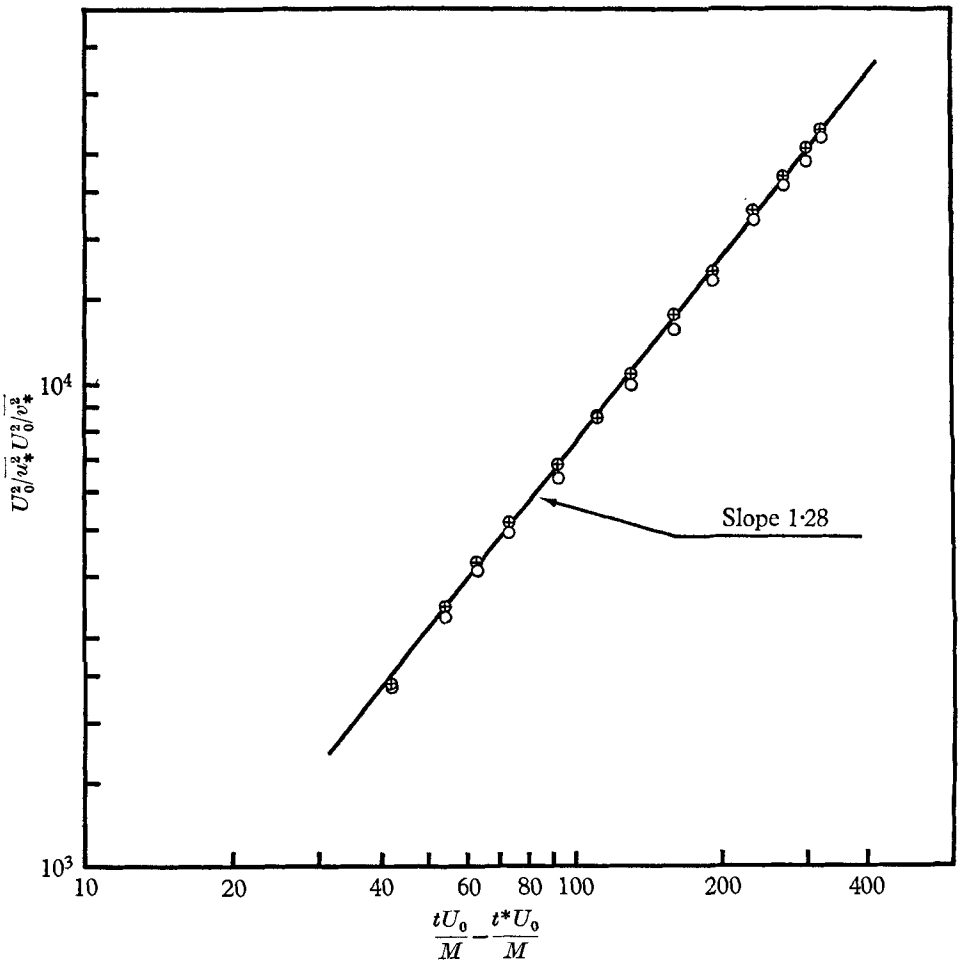

FIGURE 12. Example of u' and v' decay in a typical case after a contraction at $18M$; square-rod grid with $M = 2{\cdot}54$ cm and $U_0 = 20$ m/sec. ○, $U_0^2/\overline{u_*^2}$ with $t^*U_0/M = 4$; ⊕, $U_0^2/\overline{v_*^2}$ with $t^*U_0/M = 4$.

Location of the contraction	R_M ($\times 10^{-3}$)	U_0 (m/s)	Grid: M (cm)	Grid: σ	Grid: Type	$U_0 t^*/M$	$\overline{u^2}$-decay: n_1^*	$\overline{u^2}$-decay: A_1^*	$\overline{v^2}$-decay: n_2^*	$\overline{v^2}$-decay: A_2^*
$18M$	17	10	2·54	0·34	Biplane, square rods	3	1·29	19	1·28	18
	34	20				4	1·27	20	1·29	19
$18M$	34	10	5·08	0·34	Biplane, square rods	3·5	1·25	21	1·25	20
	68	20				3·5	1·25	22	1·27	19
$9M$	68	10	10·16	0·34	Biplane, square rods	3·5	1·17	26	1·19	24
	68	10				5	1·16	27	1·15	28
	135	20				4·5	1·15	29	1·16	28
$18M$	34	10	5·08	0·44	Biplane, round rods	4	1·24	35	1·24	34
	68	20				4	1·26	34	1·27	32
$18M$	34	10	5·08	0·31	Disks	2	1·32	7·1	1·32	7·5
	68	20				4·5	1·33	7·9	1·30	9·7

TABLE 3. Energy decay of the grid turbulence after straining by the contraction

6. A simple derivation of Kolmogorov's decay law for isotropic turbulence

At large enough Reynolds numbers, stationary turbulence with only moderate levels of mean shear seems to be well described by Kolmogorov's local-isotropy similarity theory in the large-wave-number range (Kolmogorov 1941*a*; Batchelor 1953; Grant, Stewart & Moilliet 1962; Gibson 1963). However, the Kolmogorov postulate that all statistical functions depend on only the dissipation rate ϵ and the kinematic viscosity ν is not clearly applicable to decaying (fully) isotropic turbulence. As Goldstein (1951) pointed out, if the decay is relatively rapid we might expect spectra and other functions to depend on ϵ, $d\epsilon/dt$, etc.

Nevertheless (Batchelor 1953), if the decay rate is slow enough compared with characteristic spectral times, e.g. the inertial time, apparently introduced by Onsager (1949),

$$\tau_k \equiv (k^3\mathscr{E})^{-\frac{1}{2}}, \tag{8}$$

then the stationary Kolmogorov theory may be applicable at each instant to decaying isotropic turbulence. $\mathscr{E}(k,t)$ is the three-dimensional energy spectrum, k is the wave-number. The condition

$$\tau_k(k) \ll \frac{\mathscr{E}}{|\partial\mathscr{E}/\partial t|} \tag{9}$$

is a criterion for the wave number above which a quasi-stationary theory is a reasonable approximation. t is time.

The corresponding shear-flow condition, for the wave-number above which the directional strain effect in destroying isotropy may be negligible compared with the orientation-losing cascade process, has been discussed by Corrsin (1957, 1958) and Uberoi (1957).

Kolmogorov's second principal postulate is that when the Reynolds number is large enough that viscous effects are far removed from the start in k of the locally isotropic spectral region, there will exist an inertial subrange, a k-range in which statistical functions will depend only on ϵ. The corresponding spectral form is

$$\mathscr{E} = C\epsilon^{\frac{2}{3}}k^{-\frac{5}{3}}. \tag{10}$$

For any given kind of turbulent flow, it is well known that this locally isotropic, inertial subrange should be more extensive in k as the Reynolds number increases (Batchelor 1953; Corrsin 1958). In fact, some rough theoretical estimates of gross turbulence properties at large Reynolds numbers have been found by replacing the entire turbulence spectrum by

$$\left.\begin{aligned} \mathscr{E}(k,t) = 0 \quad \text{for} \quad & \begin{cases} 0 \leqslant k \leqslant k_L, \\ k > (\epsilon/\nu^3)^{\frac{1}{4}} \equiv k_k, \end{cases} \\ \mathscr{E}(k,t) = C\{\epsilon(t)\}^{\frac{2}{3}}k^{-\frac{5}{3}} \quad & \text{for} \quad k_L \leqslant k \leqslant k_k. \end{aligned}\right\} \tag{11}$$

k_L is roughly the inverse of the integral scale of the turbulence (see Corrsin 1959, 1964).

For example, this yields an estimate $C \approx \frac{2}{3}$, which can be compared with the experimental values of about 1·5 (Grant, *et al.* 1962; Gibson 1963).

The differential equation for energy decay rate in isotropic turbulence is

$$\frac{1}{2}\frac{d\overline{q^2}}{dt} = -\epsilon, \tag{12}$$

where $q^2 \equiv u_i u_i$, the squared resultant fluctuation.

$$\tfrac{1}{2}\overline{q^2} = \int_0^\infty \mathscr{E}\, dk, \quad \text{and} \quad \epsilon = 2\nu \int_0^\infty k^2 \mathscr{E}\, dk.$$

Simple substitution of (11) into either side of (12) to seek $\overline{q^2}(t)$ or $\epsilon(t)$ is incomplete because $k_L(t)$ enters as another unknown function:

$$\tfrac{1}{2}\overline{q^2} \approx C\epsilon^{\frac{2}{3}} \int_{k_L}^{k_k} k^{-\frac{5}{3}}\, dk = \tfrac{3}{2} C\epsilon^{\frac{2}{3}}(k_L^{-\frac{2}{3}} - k_k^{-\frac{2}{3}}). \tag{13}$$

Therefore

$$\tfrac{1}{2}\overline{q^2} \approx \tfrac{3}{2}(C\epsilon^{\frac{2}{3}}/k_L^{\frac{2}{3}}), \tag{14}$$

since $k_k^{\frac{2}{3}} \gg k_L^{\frac{2}{3}}$ at large enough Reynolds numbers. An additional relation among $\overline{q^2}$, ϵ and k_L is needed.

The spectral model can be completed for this purpose by exploiting the following two known properties:

(*a*) In the neighbourhood of $k = 0$,

$$\mathscr{E}(k,t) = B(t)k^4 + \{\text{terms of higher order in } k\}. \tag{15}$$

(*b*) With (15) it is obvious that τ_k as defined in (8) becomes very large indeed as $k \to 0$.

Consequently we choose a two-range model of the spectrum consisting of a 'permanent' part ($\sim k^4$) at small k and a decaying Kolmogorov part ($\sim k^{-\frac{5}{3}}$) at larger $k \leqslant k_k$. The moving intersection of the two curves is taken to define $k_L(t)$, thereby providing the additional relation required to make the decay problem determinate (figure 13). Now we have

$$\mathscr{E}(k,t) = Bk^4 \quad \text{for} \quad 0 \leqslant k \leqslant k_L, \tag{16}$$

with $B \approx$ const., to replace the first part of equation (11).

With matching of the segments at k_L, B is expressible in terms of C, $\epsilon(t)$ and $k_L(t)$, but its constancy is the property of principal use here. The formal connexion between 'integral scale' and $\mathscr{E}$ (Batchelor 1953) can be used to show that k_L is approximately the inverse of an integral scale. The matching gives

$$B = C\epsilon^{\frac{2}{3}} k_L^{-\frac{17}{3}}. \tag{17}$$

Putting this into the two-range model, and integrating to get the energy, we find

$$\tfrac{1}{2}\overline{q^2} \approx \frac{17}{10}\frac{C\epsilon^{\frac{2}{3}}}{k_L^{\frac{2}{3}}}, \tag{18}$$

a slight improvement on (14).

Eliminating k_L between (18) and (17), we can express ϵ in terms of $\overline{q^2}$ for substitution into the decay equation. The resulting solution can be expressed as

$$1/\overline{q^2} = D(t - t_1)^{\frac{10}{7}}, \tag{19}$$

where D is a constant and t_1 is the hypothetical time at which $1/\overline{q^2} = 0$.

This is just Kolmogorov's 'decay law' (1941*b*). His derivation assumed the following:

(*a*) constancy of the 'Loitsianskii integral' (1939):

$$\int_0^\infty r^4 \mu(r,t)\,dr = \text{const.}, \tag{20}$$

where $$\mu(r,t) \equiv \overline{u_1(x_1,x_2,x_3,t)\,u_1(x_1+r,x_2,x_3,t)};$$

(*b*) the full integral-scale similarity of the correlation function insofar as the application of (20) is concerned:

$$\mu(r,t) = \overline{u_1^2}(t) f_n\{r/L(t)\}; \tag{21}$$

(*c*) the inertial subrange form of $\mu\{\sim(1-Nr^2)\}$ over an unspecified interval in r.

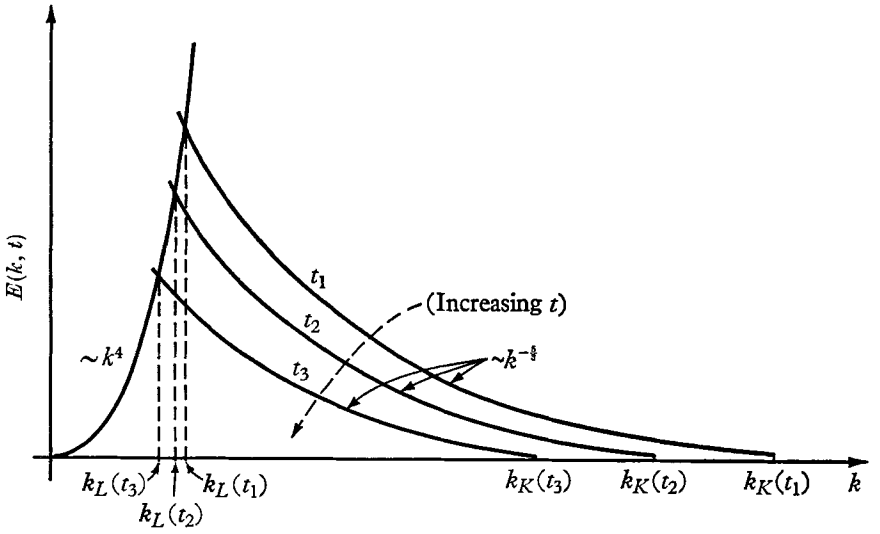

FIGURE 13. Two-range model of 'three-dimensional', isotropic inertial spectrum: schematic sketch.

The present derivation differs only in that the Kolmogorov–inertial-subrange relation ($\sim k^{-\frac{5}{3}}$) is applied over a specific spectral range and that no overall similarity statement appears. In any case the present approach seems equivalent to the original one. In further agreement, it yields

$$1/k_L \approx L \sim (t-t_1)^{\frac{2}{7}}. \tag{22}$$

From equations (17) and (18),

$$B \approx \tfrac{5}{17}\overline{q^2} k_L^{-5}, \tag{23}$$

and if B is assumed approximately constant,

$$\overline{q^2} k_L^{-5} = \text{const.}, \tag{24}$$

essentially the result of Kolmogorov deduced from (20) and (21).

It was shown by Proudman & Reid (1954) under special assumptions, and by Batchelor & Proudman (1956) more generally that the Loitsianskii integral in

principle cannot be constant. Therefore the Kolmogorov law may have received less attention than it merits. We note that $10/7 (\approx 1{\cdot}43)$ is not very far from the average empirical exponent of about 1·2 to 1·35. In fact Uberoi (1965) has reported values as large as 1·4, and our disk-grid turbulence was in that range.

The point is that even though the Loitsianskii integral cannot be constant, its change is slow enough compared with the energy decay that taking the integral (or B) constant† can still give a reasonable estimate of the decay rate. Using a time spectrum defined by (8), with $\mathscr{E} = Bk^4$ and (23) for B, and omitting numerical factors of order one, we find for the low k end of the spectrum

$$\tau_k/\tau_D \approx (k_L/k)^{\frac{7}{2}}. \tag{25}$$

$\tau_D \equiv (k_L q')^{-1}$ is the time characterizing the energy decay (Batchelor 1953). Clearly τ_k/τ_D increases rapidly as k/k_L approaches zero.

It is also interesting to seek a best power-law fit to experiments on the growth of the integral scales. Integral-scale measurements are much less numerous than those of turbulence level. We still have too few points in the present investigation to draw reliable curves, but the best power law fits of type

$$L \sim (x - x_1)^m \tag{26}$$

give the results in table 4 for 'transverse' and 'longitudinal' scales, L_g and L_f respectively. L_g and L_f refer to integrals of the von Kármán & Howarth (1938) $g(r)$ and $f(r)$ correlation-coefficient functions in isotropic turbulence:

$$L_g \equiv \int_0^\infty g(r)\,dr, \quad L_f \equiv \int_0^\infty f(r)\,dr. \tag{27}$$

In these experiments the 'g-like' correlations are all

$$\overline{u_1(x_1, x_2, x_3, t)\, u_1(x_1, x_2 + r, x_3, t)},$$

and the 'f-like' correlations are all

$$\overline{u_1(x_1, x_2, x_3, t)\, u_1(x_1 + r, x_2, x_3, t)}.$$

Some values of L_f are determined from the (extrapolated) zero-frequency intercept of u_1 spectra.

The most extensive set of values appears to be that of Dryden, Schubauer, Mock & Skramstad (1937), but the scatter in these early data is too large for slope determination. The larger-Reynolds-number cases of Batchelor & Townsend (1948) were also rather scattered.

The highly speculative conclusions which might be drawn from table 4 are:

(*a*) That the turbulence behind the grids in the *straight* ducts is not isotropic with respect to integral scales. The difference in growth rates for L_g and L_f makes it impossible for them to fulfill over appreciable distance the isotropic condition $L_f = 2L_g$ (von Kármán & Howarth 1938). On the other hand, the exponents for L_g and L_f in the turbulence strained by a slight contraction are roughly equal. It should be added that these preliminary data also show $L_f \approx 2L_g$.

† It was pointed out by Lin (1947) that B is proportional to the Loitsianskii integral.

(*b*) That the Kolmogorov $\frac{2}{7}(\doteq 0{\cdot}29)$ law may be fairly good in 'properly' strained grid turbulence.

Deeper and more complete turbulence theories, such as that of Kraichnan (1959), will be able to predict the decay rate more accurately than will the Kolmogorov law. Yet simpler, less accurate theories can be a help in both application and understanding.

Reference	R_M ($\times 10^{-3}$)	Biplane grids: Rods	Biplane grids: σ	Contraction	Integral scale	m
Corrsin (1942)	8·5	Round	0·44	No	L_g	0·53
	17	Round	0·44	No	L_g	0·49
Batchelor & Townsend (1948)	2·8	Round	0·34	No	L_g	0·44
Uberoi & Corrsin (1953)	13·2	Round	0·44	No	L_g	0·48
	6·6	Round	0·44	No	L_g	0·52
Mills, Kistler, O'Brien & Corrsin (1957)	7·3	Round	0·44	No	L_f	0·30
Present work	68	Square	0·34	No	L_f	0·34
	34	Square	0·34	Yes	L_g	0·40
	68	Square	0·34	Yes	L_f	0·35

TABLE 4. Power-law exponent for integral-scale growth.

A few words should be added about other simple, explicit decay estimates. The earliest is that of Taylor (1935*b*), whose key assumption was *constancy of the integral scales*. This leads to

$$1/\overline{q^2} \sim (t-t_1)^2. \tag{28}$$

Dryden (1943) carried the von Kármán–Howarth (1938) similarity analysis a step beyond the original authors by retaining the viscous term in the two-point correlation equation, and observing that the only result consistent with full similarity is

$$1/\overline{q^2} \sim (t-t_1), \quad L \sim (t-t_1)^{\frac{1}{2}}, \tag{29}$$

and (necessarily for any complete similarity) constant Reynolds number,

$$q'L/\nu = \text{const.} \tag{30}$$

Equation (29) has since been re-derived by others from a number of different starting-points. It gives fair agreement with experiment in grid turbulence over a limited distance and is taken by Batchelor (1953) to apply to the 'initial period'. But any data which follow a smooth curve can be fitted over some distance by a straight line. In the previous sections we have seen that $1/\overline{u^2} \sim (x-x_1)^n$ fits the data over the largest distance for n somewhere between 1·2 and 1·3. This seems a more accurate, empirical 'initial period' decay law.

With a partial similarity assumption Lin (1948) arrived at a form somewhat like (29), but with an additional empirical constant. This permits a better fit to the experiments.

It should be remarked parenthetically that Deissler's (1960) computation of isotropic turbulence decay, with the 'correlation-discard' method of truncating

the infinite hierarchy of moment equations, gives values of n and m which are roughly 1·3 and 0·4 if we use his figures 8 and 13, and select the common time origin which provides the longest pair of straight lines on log–log plots. Since this correlation-discard approximation is valid at most for small Reynolds numbers, and can lead to negative energy spectra (Kraichnan 1963), the plausible values of n and m cannot be taken as confirmation in principle of the approximation.

7. Justification for comparing steady grid turbulence with isotropic turbulent theories

Since the connexion was begun by Taylor (1935*b*), it has been customary to compare theories of (necessarily non-stationary) isotropic turbulence with wind-tunnel measurements of (stationary) inhomogeneous turbulence behind grids. The technique of comparison is the assumption that time derivatives in a co-ordinate system travelling with the mean speed in the grid turbulence, i.e.

$$\left\{\frac{\partial(^-)}{\partial t}\right\}_{\substack{\text{following}\\ \text{mean motion}}} \equiv \overline{U}\frac{d(^-)}{dx},$$

can be identified with the time derivatives at a fixed point in truly isotropic turbulence having zero mean speed.

Perhaps the first quantitative justification for such an approximation was the observation that the grid turbulence is indeed approximately isotropic (MacPhail 1940). Furthermore, it turns out (Corrsin 1963*a*) that a number of dimensionless measures of inhomogeneity due to decay

$$\frac{L_f}{\overline{u^2}}\frac{d\overline{u^2}}{dx}, \quad \frac{L_f}{\lambda}\frac{d\lambda}{dx}, \quad \frac{dL_f}{dx}$$

are fairly small compared to unity for $x/M > 40$. λ is a 'Taylor microscale'.

A slightly different view of the point is given by a rough estimate of the effect of differential transport of turbulent energy down the gradient. The turbulent energy equation in the transversely homogeneous region far behind a grid can be crudely represented by

$$\overline{U}\frac{d\overline{q^2}}{dx} \approx -2\epsilon - \frac{d}{dx}\left(\mathscr{D}\frac{d\overline{q^2}}{dx}\right). \tag{31}$$

Here $\frac{1}{2}q^2 \equiv \frac{1}{2}u_i u_i$, the turbulent energy per unit mass, ϵ is the viscous dissipation rate, and the last term (presumably small) is the net change in $\frac{1}{2}\overline{q^2}$ due to energy flux. There is energy flux due to turbulent convection, pressure-gradient work and viscous forces. The third of these is negligible relative to the first (Uberoi & Corrsin 1953). For an order of magnitude estimate, we suppose the transport term to represent both turbulence effects, and we approximate the 'turbulent diffusivity' as

$$\mathscr{D} \approx u' L_f, \tag{32}$$

an estimate which includes the replacing of an inherently Lagrangian scale by an Eulerian one (Corrsin 1963*b*).

With ϵ replaced by the estimate in terms of integral scale, q'^3/L_f (Taylor 1935*b*, Batchelor 1953), and with $d\overline{q^2}/dx$ in the small term replaced by its value in (31) with the small term $-2\epsilon/\overline{U}$ neglected we can calculate the relative order

$$\frac{1}{2}\left|\frac{d}{dx}\left(\mathscr{D}\frac{d\overline{q^2}}{dx}\right)\right| \Big/ \epsilon \approx \frac{\overline{q^2}}{\overline{U}^2} \ll 1. \tag{33}$$

We conclude that the effect of inhomogeneity-induced energy transfer on the decay rate is slight.

8. A possible mechanism for energy inequality

The new data reported here indicate that the condition $\overline{u^2} \approx \overline{v^2}$ is retained after being forced by a contraction. The results of Uberoi & Wallis (1964), however, and the obvious fact that the inhomogeneous turbulence cannot be exactly isotropic both suggest a search for an explicit mechanism which might under some conditions tend to restore the inequality $\overline{u^2} > \overline{v^2}$.

The steady-state component-energy equations are

$$\tfrac{1}{2}\overline{U}_k\frac{\partial\overline{u^2}}{\partial x_k} = -\overline{u_i u}\frac{\partial\overline{U}}{\partial x_i} - \frac{1}{2}\frac{\partial}{\partial x_j}\overline{(u_j u^2)} - \frac{1}{\rho}\overline{u\frac{\partial p}{\partial x}} + \nu\overline{u\nabla^2 u}, \tag{34}$$

$$\tfrac{1}{2}\overline{U}_k\frac{\partial\overline{v^2}}{\partial x_k} = -\overline{u_i v}\frac{\partial\overline{V}}{\partial x_i} - \frac{1}{2}\frac{\partial}{\partial x_j}\overline{(u_j v^2)} - \frac{1}{\rho}\overline{v\frac{\partial p}{\partial y}} + \nu\overline{v\nabla^2 v}. \tag{35}$$

In this mixed notation $u \equiv u_1$, $v \equiv u_2$ or u_3, $x \equiv x_1$, $y \equiv x_2$ or x_3.
Since we shall restrict attention to axially symmetric turbulence, the $\overline{v^2}$ equation can represent $\overline{w^2}$ as well.

For the special case with rectilinear mean flow in the x-direction, and transverse homogeneity these simplify to

$$\tfrac{1}{2}\overline{U}\frac{d\overline{u^2}}{dx} = -\frac{1}{2}\frac{d\overline{u^3}}{dx} - \frac{1}{\rho}\overline{u\frac{\partial p}{\partial x}} + \nu\overline{u\nabla^2 u}, \tag{36}$$

$$\tfrac{1}{2}\overline{U}\frac{d\overline{v^2}}{dx} = -\frac{1}{2}\frac{d}{dx}\overline{uv^2} - \frac{1}{\rho}\overline{v\frac{\partial p}{\partial y}} + \nu\overline{v\nabla^2 v}. \tag{37}$$

The static pressure terms exchange energy among velocity directional components (see, for example, Batchelor 1953). It is generally believed, though possibly not theoretically deducible from the equations of motion, that they tend to transfer energy from more energetic to less energetic components. With inhomogeneity, they also transport energy. The viscous terms include both dissipation and transport. The former destroys component energy at a rate proportional to that energy, hence it is unlikely to enhance or create an inequality. The latter will be negligible compared with the turbulent transport (Uberoi & Corrsin 1953). Therefore the most likely possibility for generation of energy inequality is a difference in turbulent transport of component energies, the two first terms on the right sides of (36) and (37). For isotropic turbulence $\overline{u^3}$ and $\overline{uv^2}$ are both identically zero. In grid-generated turbulence in a straight channel measure-

ments show $\overline{u^3}$ negligible† and, although $\overline{uv^2}$ does not seem to have been measured, it is probably negligible as well. Estimates follow shortly.

However, one of the principal results of the contraction studies was the growth of $|\overline{u^3}|/\overline{u^2}^{\frac{3}{2}}$ due to the strain (Mills & Corrsin 1959). In a 4 : 1 contraction this grew to 0·08. Furthermore, it returned rapidly to zero in the straight section following the contraction. From (36) it is clear that such a gradient in $\overline{u^3}$ will affect $\overline{u^2}$.

We have no data on $\overline{uv^2}$ in contractions. However, a crude theoretical estimate was successful for $\overline{u^3}$ due to strain, so a similar analysis may be satisfactory for estimating $\overline{uv^2}$. Following Mills & Corrsin (1959), we deduce an approximate, steady-state equation for $\overline{u^3}$:

$$\tfrac{1}{3}\overline{U}\frac{\partial\overline{u^3}}{\partial x} \approx -\overline{u^3}\frac{\partial\overline{U}}{\partial x} - \frac{1}{3}\frac{\partial\overline{u^4}}{\partial x} + \frac{1}{2}\frac{\partial}{\partial x}\overline{u^2}^2 - \frac{1}{\rho}\overline{u^2\frac{\partial p}{\partial x}} + \nu\overline{u^2\nabla^2 u}. \tag{38}$$

The u-equation is found by subtracting the averaged x-component Navier–Stokes equation from the unaveraged one, in the manner of Reynolds. The u-equation is then multiplied by u^2 and averaged. Equation (38) results under the following assumptions:

$$\left.\begin{aligned} \left|\overline{V}\frac{\partial\overline{u^3}}{\partial y}\right| &\ll \left|\overline{U}\frac{\partial\overline{u^3}}{\partial x}\right|, \quad \left|\overline{u^2v}\frac{\partial\overline{U}}{\partial y}\right| \ll \left|\overline{u^3}\frac{\partial\overline{U}}{\partial x}\right|; \\ \left|\frac{\partial}{\partial y}\overline{u^3v}\right| &\ll \left|\frac{\partial}{\partial x}\overline{u^4}\right|, \quad \left|\frac{\partial\overline{uv}}{\partial y}\right| \ll \left|\frac{\partial\overline{u^2}}{\partial x}\right|. \end{aligned}\right\} \tag{39}$$

From the u- and v-momentum equations, we can deduce one for $\overline{uv^2}$:

$$\overline{U}\frac{\partial\overline{uv^2}}{\partial x} \approx -\frac{\partial}{\partial x}\overline{u^2v^2} + \overline{v^2}\frac{\partial\overline{u^2}}{\partial x} - \frac{1}{\rho}\overline{v^2\frac{\partial p}{\partial x}} - \frac{2}{\rho}\overline{uv\frac{\partial p}{\partial y}} + \nu(2\overline{uv\nabla^2 v} + \overline{v^2\nabla^2 u}). \tag{40}$$

The largest mean-strain-rate terms in (40) have cancelled out by continuity. We have neglected the remaining mean-strain-rate terms such as $\overline{v^3}\,\partial\overline{U}/\partial y$ by comparison with the mean-strain-rate term in (38).

Equations (38) and (40) can be exploited to estimate $\overline{u^3}$ and $\overline{uv^2}$ at the end of a weak, rapid contraction, supposing the entering turbulence is virtually isotropic To pare the analysis down as much as possible, we (*a*) neglect the viscous terms; (*b*) neglect the pressure terms because they are zero in the entering flow; (*c*) suppose $\overline{u^4} \approx 3\overline{u^2}^2$ and $\overline{u^2v^2} \approx \overline{u^2}\,\overline{v^2}$. This 'Millionstchikov hypothesis' is known to lead to trouble in some problems (Kraichnan 1963).

The residual equations are, using total derivatives in this approximation,

$$\overline{U}\frac{d\overline{u^3}}{dx} \approx -3\,\overline{u^3}\frac{d\overline{U}}{dx} - 3\overline{u^2}\frac{d\overline{u^2}}{dx}, \tag{41}$$

$$\overline{U}\frac{d\overline{uv^2}}{dx} \approx -\overline{u^2}\frac{d\overline{v^2}}{dx}. \tag{42}$$

† $|\overline{u^3}/(\overline{u^2})^{\frac{3}{2}}|$ is so small ($< 0{\cdot}002$) as to be submerged in the noise level of standard hot-wire equipment (Mills & Corrsin 1959). P. S. Klebanoff & F. N. Frenkiel (private communication) have recently found a much larger value, $\approx 0{\cdot}03$, but this would not change the conclusions here.

The corresponding crude equations for $\overline{u^2}$- and $\overline{v^2}$-changes in the contraction, where mean-strain effects dominate, are

$$\overline{U}\frac{d\overline{u^2}}{dx} \approx -2\overline{u^2}\frac{d\overline{U}}{dx}, \tag{43}$$

$$\overline{U}\frac{d\overline{v^2}}{dx} \approx \overline{v^2}\frac{d\overline{U}}{dx}. \tag{44}$$

With these, (41) and (42) can be solved for $\overline{u^3}$ and $\overline{uv^2}$ in terms of $\overline{U}(x)$ and the pre-contraction values, $\overline{U}_p, \overline{u_p^2}, \overline{v_p^2}$:

$$\overline{u^3} \approx 3\frac{\overline{u_p^2}^2\,\overline{U}_p^2}{\overline{U}^3(x)}\left(1-\frac{\overline{U}_p^2}{\overline{U}^2(x)}\right), \tag{45}$$

$$\overline{uv^2} \approx -\frac{1}{2}\frac{\overline{u_p^2}\,\overline{v_p^2}}{\overline{U}_p}\left(1-\frac{\overline{U}_p^2}{\overline{U}^2(x)}\right). \tag{46}$$

The relevant dimensionless coefficients are expressible as

$$\frac{\overline{u^3}}{\overline{u^2}^{\frac{3}{2}}} \approx 3\frac{u_p'}{\overline{U}_p}\left(1-\frac{\overline{U}_p^2}{\overline{U}^2(x)}\right), \tag{47}$$

$$\frac{\overline{uv^2}}{u'\overline{v^2}} \approx -\frac{1}{2}\frac{u_p'}{\overline{U}_p}\left(1-\frac{\overline{U}_p^2}{\overline{U}^2(x)}\right). \tag{48}$$

Now the $\overline{u^3}$ and $\overline{uv^2}$ at the end of our contraction can be estimated. Since $\overline{U} \to 1{\cdot}27\overline{U}_p$ and $u_p'/\overline{U}_p \approx 0{\cdot}03$ (for cases with the contraction at $U_0 t/M = 18$),

$$\left.\begin{aligned}\overline{u_c^3}/\overline{u_c^2}^{\frac{3}{2}} &= 0{\cdot}034,\\ \overline{u_c v_c^2}/u_c'\overline{v_c^2} &= -0{\cdot}006.\end{aligned}\right\} \tag{49}$$

In order to use these numbers to estimate an order of energy inequality due to differential energy transport, we simplify (36) and (37) to

$$\tfrac{1}{2}\overline{U}\frac{d\overline{u^2}}{dx} \approx -\frac{1}{2}\frac{d\overline{u^3}}{dx}, \tag{50}$$

$$\tfrac{1}{2}\overline{U}\frac{d\overline{v^2}}{dx} \approx -\frac{1}{2}\frac{d\overline{uv^2}}{dx}. \tag{51}$$

These should give an upper bound on the growth of anisotropy for reasons mentioned after (36) and (37).

Where $\overline{u^3}$ and $\overline{uv^2}$ have become again sensibly zero, an empirical event in the straight section following the contraction,

$$\overline{u_s^2} \approx \overline{u_c^2} + \overline{u_c^3}/\overline{U}_c, \tag{52}$$

$$\overline{v_s^2} \approx \overline{v_c^2} + \overline{u_c v_c^2}/\overline{U}_c. \tag{53}$$

With $\overline{v_c^2} = \overline{u_c^2}$, a relevant dimensionless form is

$$\frac{\overline{u_s^2} - \overline{v_s^2}}{\overline{u_c^2}} \approx \frac{u_c'}{U_c}\left(\frac{\overline{u_c^3}}{\overline{u_c^2}^{\frac{3}{2}}} - \frac{\overline{u_c v_c^2}}{u_c' \overline{v_c^2}}\right). \tag{54}$$

This result yields the sign reported by Uberoi but, with the numerical values of (49), the effect is quite negligible—consistent with the present experiments.

We should like to thank Bernard Baker for his care in making the grids and the traversing apparatus, and Yi-shuong Kuo for his help in the laboratory. This work was supported by the U.S. National Science Foundation, Grant G 21505.

REFERENCES

BAINES, W. D. & PETERSON, E. G. 1951 An investigation of flow through screens. *Trans. Amer. Soc. Mech. Engr.* **73**, 467.

BATCHELOR, G. K. 1953 *The Theory of Homogeneous Turbulence.* Cambridge University Press.

BATCHELOR, G. K. & PROUDMAN, I. 1954 The effect of rapid distortion of a fluid in turbulent motion. *Quart. J. Mech. Appl. Math.* **7**, 83.

BATCHELOR, G. K. & PROUDMAN, I. 1956 The large-scale structure of homogeneous turbulence. *Phil. Trans.* A, **248**, 396.

BATCHELOR, G. K. & STEWART, R. W. 1950 Anisotropy of the spectrum of turbulence at small wave-numbers. *Quart. J. Mech. Appl. Math.* **3**, 1.

BATCHELOR, G. K. & TOWNSEND, A. A. 1947 Decay of vorticity in isotropic turbulence. *Proc. Roy. Soc.* A, **190**, 534.

BATCHELOR, G. K. & TOWNSEND, A. A. 1948 Decay of isotropic turbulence in the initial period. *Proc. Roy. Soc.* A, **193**, 539.

COMTE-BELLOT, G. & MATHIEU, J. 1958 Sur la détermination expérimentale des coefficients de sensibilité aux fluctuations de vitesse et de température des anémomètres à fil chaud. *C.R. Acad. Sci., Paris*, **246**, 3219.

COMTE-BELLOT, G. 1960 Valeurs efficaces, coefficients de dissymetrie et d'aplatissement des fluctuations transversales de vitesse dans un tunnel bidimensionnel à parois parallèles. *C.R. Acad. Sci., Paris*, **251**, 2656.

CORRSIN, S. 1942 Decay of turbulence behind three similar grids. Aero Eng. Thesis, California Institute of Technology.

CORRSIN, S. 1957 Some current problems in turbulent shear flows. *Symposium on Naval Hydrodynamics*, chap. 15. Publ. 515 of Nat. Acad. Sci.-Nat. Res. Council, Washington.

CORRSIN, S. 1958 Local isotropy in turbulent shear flow. *NACA R & M* 58B11.

CORRSIN, S. 1959 Outline of some topics in homogeneous turbulent flow. *J. Geophys. Res.* **64**, 2134.

CORRSIN, S. 1963*a* Turbulence: experimental methods. *Handbuch der Physik*, vol. VIII/2, (eds. S. Flugge and C. A. Truesdell). Berlin: Springer.

CORRSIN, S. 1963*b* Estimates of the relations between Eulerian and Lagrangian scales in large Reynolds number turbulence. *J. Atmos. Sci.* **20**, 115.

CORRSIN, S. 1964 The isotropic turbulence mixer: Part II. *Amer. Inst. Chem. Engr. J.* **10**, 870.

DEISSLER, R. G. 1960 A theory of decaying homogeneous turbulence. *Phys. Fluids*, **3**, 176.

DRYDEN, H. L. 1943 A review of the statistical theory of turbulence. *Quart. Appl. Math.* **1**, 7.

DRYDEN, H. L., SCHUBAUER, G. B., MOCK, W. C. & SKRAMSTAD, H. K. 1937 Measurements of the intensity and scale of wind tunnel turbulence and their relation to the critical Reynolds number of spheres. *NACA Rep.* no. 581.

DUMAS, R. 1964 Contribution a l'étude des spectres de turbulence. *Pub. Sci. Tech. Min. de l'Air, Paris*, no. 404.

GIBSON, M. M. 1963 Spectra of turbulence in a round jet. *J. Fluid Mech.* **15**, 161.

GOLDSTEIN, S. 1951 On the law of decay of homogeneous isotropic turbulence and the theories of the equilibrium and similarity spectra. *Proc. Camb. Phil. Soc.* **47**, 554.

GRANT, H. L. & NISBET, I. C. T. 1957 The inhomogeneity of grid turbulence. *J. Fluid Mech.* **2**, 263.

GRANT, H. L., STEWART, R. W. & MOILLIET, A. 1962 Turbulence spectra from a tidal channel. *J. Fluid. Mech.* **12**, 241.

VON KÁRMÁN, T. & HOWARTH, L. 1938 On the statistical theory of isotropic turbulence. *Proc. Roy. Soc.* A, **164**, 192.

KISTLER, A. L. & VREBALOVICH, T. 1961 Turbulence measurements at the 8 by 10-foot Cooperative Wind Tunnel. *Jet Prop. Lab. Res. Summary*, no. 36-4, 12 (also private communication).

KOLMOGOROV, A. N. 1941*a* The local structure of turbulence in incompressible viscous fluid for very large Reynolds numbers. *C.R. Akad. Sci. SSSR (Dok.)*, **30**, 301.

KOLMOGOROV, A. N. 1941*b* On degeneration of isotropic turbulence in an incompressible viscous liquid. *C.R. Akad. Sci. SSSR (Dokl.)*, **31**, 538.

KRAICHNAN, R. H. 1959 The structure of isotropic turbulence at very high Reynolds numbers. *J. Fluid Mech.* **5**, 497.

KRAICHNAN, R. H. 1963 Direct-interaction approximation for a system of several interacting simple shear waves. *Phys. Fluids*, **6**, 1603.

LIN, C. C. 1947 Remarks on the spectrum of turbulence. *Proc. 1st Symp. Appl. Math.* New York: McGraw-Hill.

LIN, C. C. 1948 Note on the law of decay of isotropic turbulence. *Proc. Nat. Acad. Sci.* **34**, 540.

LOITSIANSKII, L. G. 1939 Some basic laws of isotropic turbulent flow. *Cent. Aero. Hydro. Inst., Moscow, Rep.* no. 440. (Translation in *NACA TM* no. 1079.)

MACPHAIL, D. C. 1940 An experimental verification of the isotropy of turbulence produced by a grid. *J. Aero Sci.* **8**, 73.

MILLS, R. R. & CORRSIN, S. 1959 Effect of contraction on turbulence and temperature fluctuations generated by a warm grid. *NASA Memo* 5-5-59W.

MILLS, R. R., KISTLER, A. L., O'BRIEN, V. & CORRSIN, S. 1958 Turbulence and temperature fluctuations behind a heated grid. *NACA TN* no. 4288.

ONSAGER, L. 1949 Statistical hydrodynamics. *Nuovo Cim.* **6**, 279.

PRANDTL, L. 1932 Herstellung einwandfreier Luftströme (Windkanale). *Handbuch der Exp. Physik, Leipzig.* (Translated in *NACA TM* no. 726.)

PROUDMAN, I. & REID, W. H. 1954 On the decay of a normally distributed and homogeneous turbulent velocity field. *Phil. Trans.* A, **247**, 163.

RIBNER, H. S. & TUCKER, M. 1953 Spectrum of turbulence in a contracting stream. *NACA Rep.* no. 1113. (Originally *NACA TN* no. 2606.)

SIMMONS, L. F. G. & SALTER, C. 1934 Experimental investigation and analysis of the velocity variations in turbulent flow. *Proc. Roy. Soc.* A, **145**, 212.

TAYLOR, G. I. 1935*a* Turbulence in a contracting stream. *Z. Angew. Math. Mech.* **15**, 91.

TAYLOR, G. I. 1935*b* Statistical theory of turbulence, parts I and II. *Proc. Roy. Soc.* A, **151**, 421.

TOWNSEND, A. A. 1954 The uniform distortion of homogeneous turbulence. *Quart. J. Mech. Appl.* **7**, 104.

TSUJI, H. & HAMA, F. R. 1953 Experiment on the decay of turbulence behind two grids. *J. Aero. Sci.* **20**, 848.

UBEROI, M. S. 1956 The effect of wind tunnel contraction on free stream turbulence. *J. Aero. Sci.* **23**, 754.

UBEROI, M. S. 1957 Equipartition of energy and local isotropy in turbulent flows. *J. Appl. Phys.* **28**, 1165.

UBEROI, M. S. 1963 Energy transfer in isotropic turbulence. *Phys. Fluids*, **6**, 1048.

UBEROI, M. S. 1965 Effect of grid geometry on turbulence decay (abstract). *Bull. Am. Phys. Soc.* **10**, 265.

UBEROI, M. S. & CORRSIN, S. 1953 Diffusion of heat from a line source in isotropic turbulence. *NACA Rep.* no. 1142. (See also *NACA TN* no. 2710.)

UBEROI, M. S. & WALLIS, S. 1964 Realization of isotropic turbulence (abstract), *Bull. Amer. Phys. Soc.* **9**, 584.

UBEROI, M. S. & WALLIS, S. 1966 Small axisymmetric contraction of grid turbulence. *J. Fluid Mech.* **24**, 539.

WYATT, L. A. 1955 Energy and spectra in decaying homogeneous turbulence. Ph.D. Thesis, University of Manchester.